Sudan University of Science and Technology

College of Graduate Studies

Assessment of Radiation Dose Received during Thoraco-lumbar and Skull Examinations in Red Sea State Medical centers

تقييم الجرعة الاشعاعية اثناء فحص الجمجمة و الفقرات القطنية في المراكز الطبية بولاية البحر الاحمر

A Thesis submitted for Partial Fulfillment for the requirement of (M.Sc) Degree in Medical Physics

By:

AyadNabil Faris

Supervisor:

Ahmed MostafaAbukonna

August 2016

الآية ألمقدسه

بسم الأب والابن والروح القدس الإله الواحد
أمين

(اله السماء يعطينا النجاح ونحن عبيدة نقوم ونبني)
نحميا 20:2

DEDICATION

I dedicate this research to my:

Parents...

Family …

Friends …

Acknowledgement

First of all, I thank Allah the Almighty for helping me complete this research. I thank Dr. Ahmed MostafaAbukonna**,** my supervisor, for his help and guidance.

I would like to express my gratitude to Mr. SuhaibAlameen and the whole staff of the radiology departments in Red Sea hospitals for their great help and support.

Finally I would like to thank everybody who helped me to prepare and finish this study.

ABSTRACT

The main objective of this study was to assess patient dose during x-ray examination of skull and thoraco-lumbar in Red Sea state Hospitals. The dose received by 146 adult patients was measured using CALDOSE software by entering the parameters: focus to detector distance FDD, mAs , KVP.

The result of the study showed that the mean of ESAK were found to be (0.79 ± 0.30) for skull and (0.37 ± 0.2) for thoraco-lumbar. The INAK were found to be (0.52 ± 0.14) for thoracic lumbar and (0.67 ± 0.25) for skull. The RCI were found to be (0.39 ± 0.19) for skull and (1.04 ± 0.75) for thoraco-lumbar.

The mean ESAK values obtained are found to be within the standardreference. The data obtained may add to the available information in nationalrecords for general use. It may provide guidance on where efforts on dosereduction will need to be directed to fulfill the requirements of the optimizationprocess and serve as a reference for future researches.

Tables ofContents

List oftables

List offigures

List ofabbreviations

Abbreviation	Phrase
FDD	focus to detector distance
ESAK	Entrancesurface air kerma
KVP	Kilovoltagepeak
mAs	Millieamperesecond
INAK	Incident air kerma
RCI	Risk of cancer incidence
ICRP	InternationalCommissionOnradiationprotection
CT	Computed tomography
IAEA	InternationalAtomicEnergyAgency
TLD	Thermoluminescencedosimeter
HVL	half value layer
SSD	Surfaceskindistance
QC	Qualitycontrol
MeV	Mega electron volt
DDREF	dose and dose-rate effectiveness factor

ESD	entrance skin dose
FSD	focus to skin distance
BSF	back scatter factor
DRL	Diagnostic Reference level
NRPB	National radiation protection board
CCs	conversion coefficients
AKAP	Air Kerma Area Product

CHAPTER ONE

1. Introduction:

X-rays are high-energy photons produced by the interaction of charged particles with matter. X-rays and gamma rays have essentially the same properties but differ in origin. X-rays are either produced from a change in the electron structure of the atom or are machine produced. They are emitted from processes outside the nucleus, while gamma rays originate inside the nucleus. They also are generally lower in energy and therefore less penetrating than gamma rays. A few millimeters of lead can stop x-rays.(M.R. Deevband3, S. Saber5 2000)

Literally thousands of x-ray machines are used daily in medicine and industry for examinations, inspections, and process controls. Because of their many uses, x-rays are the single largest source of man-made radiation exposure.

Diagnostic x-ray is an acceptance imaging modality for the diagnostic of pathological conditions in both children and adult. However, x-ray have inherent hazards that are of special concern when applied to young children.(M.R. Deevband3, S. Saber5 2000)

In the context of trauma similar principles apply to imaging both the Thoracic spine (T-spine) and the Lumbar spine (L-spine). The plain X-ray anatomy and appearances of injuries to both these areas are discussed together.

Incorrect management of patients with spinal injury may lead to, or exacerbate, neurological deficit. Therefore patients with suspected spinal injury should be managed by experienced clinicians in accordance with

local and national clinical guidelines. Imaging should not delay resuscitation.

Good views of the T-spine and L-spine are difficult to achieve in the context of trauma. Clinical assessment is also often limited by distracting injuries or reduced consciousness. The clinico-radiological assessment of suspected T-spine or L-spine injuries therefore depends on careful consideration of both the clinical and radiological findings.(healthline .com).

X-rays are rarely indicated for detection of skull fractures. If there is a history of sufficient force to result in suspected fracture then CT is usually required. CT is necessary to look for underlying intracranial haemorrhage.

In the hundred years or so that following, this basic x-ray technology has become akey element in the identification, diagnostic and treatment of many type of medical problems. Today, there are different kinds of x-ray that are used for specific purposes.

Like all x-ray, this test uses a small amount of radiation, so it may not be recommended for pregnant women or small children.(Sudan Atomic Energy Commission).

1.1 Problem of the study:

Radiation is a major risk in diagnostic and therapeutic medical imaging. The fluctuation of mAs and Kvp factors can cause many problems in patients dose , and different habits to technologies can cause many problems to patients .

Most of these clinics only take in account the image quality without taking care about patient dose escpitialy the radiation exposure here is

closer to sensitive tissues and in most workers there is a limitation in knowledge of the harm effects of ionizing radiation and the lack of knowledge of the persons working with radiation about the basic principles of radiation protection and physical variables that control the dose and distribution within the patient to give a high quality image in order to minimize the patient dose and increase the image quality and all clinical in Sudan use same protocol(Kv,mAs and pitch) to children and adults patient without take age and body weight in consideration.

1.2general Objective of the study:

Tomeasure dose received during thoracic lumbar and skull conventional X-ray examinations in Red Sea State centers.

1.3 Specific objective:

1. To estimate the patient effective dose.
2. To identify the variation of radiation dose in different centers.
3. To compare the result with the local diagnostic reference level (DRL).

1.3 Significance of the study:

Radiation dose to patients and its management have become important considerations in conventional x ray imaging procedures, This study is concerned with the assessment of radiation dose for patients during x-ray examinations for skull and thoracic lumbar tests in Red Sea State centers.

1.4 Overview of the study:

This study is concerned with the assessment of radiation dose for patients during x.ray examinations for skull and thoracic lumbartests in Red Sea State centers Accordingly, it is divided into the five chapters. Chapter one is the introduction to this study. This chapter presents the historical background and radiation risks, in addition to study problem, objectives

and scope of the work. Chapter two contains the background material for the study. This chapter also includes a summary previous work performed in this field. Chapter three describes the materials and methods that used to measure dose for x.ray machines and explains in details the methods for calculation and optimization. Chapter four presents the results of this study.Chapterfive presents the discussion, conclusion and recommendations of this study and presents the suggestions for future work.

CHAPTER TWO

Theoretical Background and literature review

The X-rays were accidentally discovered in 1895, when William C. Roentgen (Figure 2.1) was experimenting with a cathode ray tube.

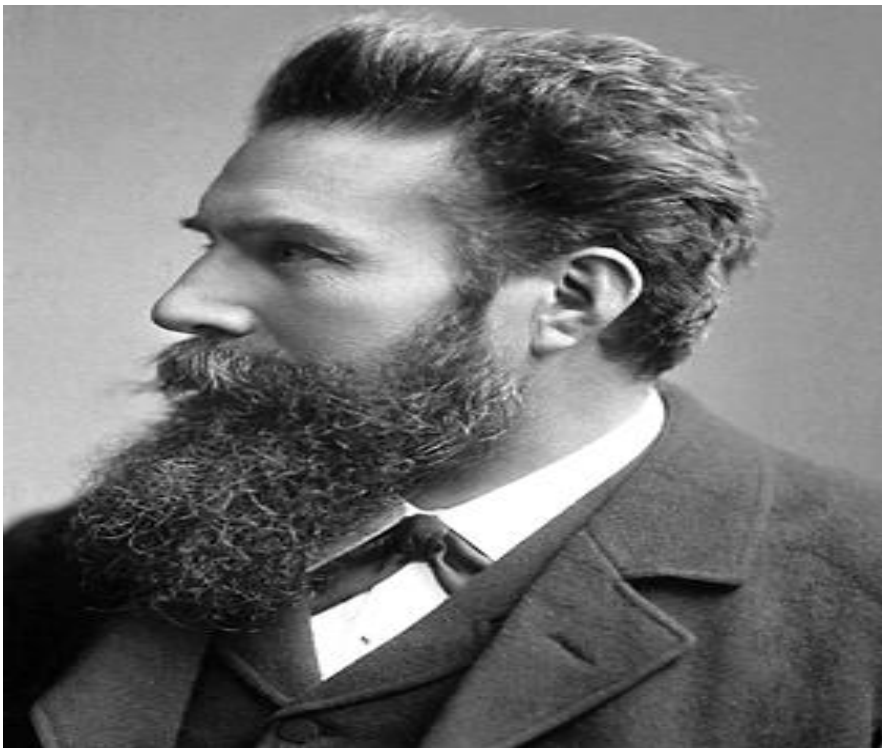

Figure2.1:WilliamC.Roentgen.(ar-encyclopedia.blogspot 2010).

Roentgen was working in his laboratory at Würzburg University in Germany. He had darkened his laboratory and completely enclosed his tube with a black paper so that he could better visualize the effects of the cathode rays in the tube (Curry 1984). A plate coated with barium platinocyanide (a fluorescent material) happened to be laying on a bench top several feet from the tube he was using. No visible light escaped from his tube because of the black paper enclosing the tube, but Roentgen noted that the barium platinocyanide fluoresced regardless of its distance from the tube (Curry 1984). Because the cathode rays Roentgen was

studying could not travel more than a few centimeters in air, he concluded that the source of that glow of the plate he noted was another kind of unknown rays. He called these unknown rays as X-rays.

Roentgen started different objects between the tube and the fluorescent plate and was able to study several characteristics of X-rays. He was able to publish and reproduce his work and was awarded in 1901 the first Nobel Prize in physics (Hendee et al., 1992). Roentgen recognized the value of his discovery to medicine and was able to produce and publish the first medical. X-ray image, the image of his wife's hand (figure 2.2) in 1896. This discovery of X-ray and its application in medicine paved the way for a new field of medicine called now radiology or diagnostic radiology (Curry et al., 1984).

Figure 2.2: Roentgen's wife hand. (rudaw.net 2015)

X-rays now play an important role in health life of all communities, Its examinations are now the most common examination in all hospitals. X rays are very high frequency electromagnetic radiation or photons. They can be counted individually using Geiger counter which make them seem like particles, But at the same time they diffract like waves when directed at a crystal. This means that X-rays can be treated as particles (photons)

or as 6 waves energy of the wave is dependent on its wavelength λ and the energy of the particle is dependent on its momentum p (Bushong 1993).Thus the energy of a photon (As a wave) (See figure 2.3) may be described either by the equation:

$$E = h\,v = h\,c / \lambda \qquad 2.1 \text{ (Curry, et al,. 1984)}$$

Where E is the energy, h is plank's constant, ν is the frequency, c is the speed of light and λ is the wavelength.

Or (as a particle) (see figure 2.4) by the equation:

$$E = P\,C \qquad 2.2 \text{ (Curry, et al,. 1984)}$$

Where m is the mAs of the particle and p is its momentum.

$$P = h / y \qquad 2.3 \text{ (Curry, et al,. 1984)}$$

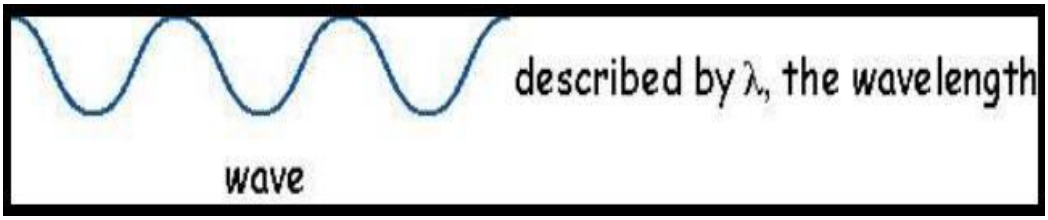

Fig 2.3 the photon as the wave (Curry, et al,. 1984)

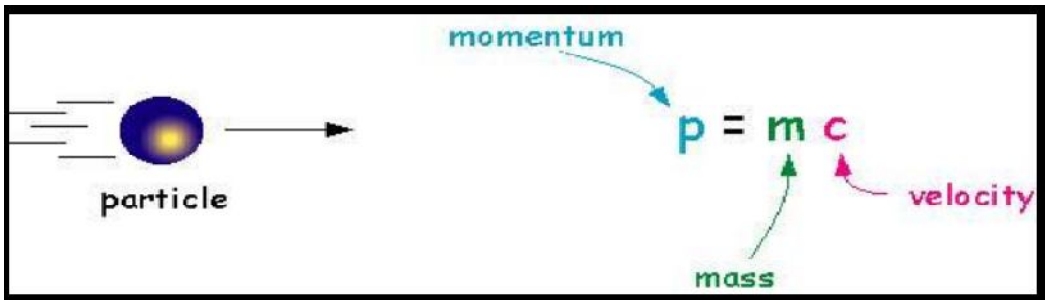

Figure 2.4 the photon as the particle (Curry, et al,. 1984)

X-rays have many properties in common with light. However, the unique properties of X-rays are what make them invaluable in diagnostic imaging. The X-rays are able to penetrate material that absorb or reflect light. When X-rays are absorbed by a certain material, they may produce light. Like light, X-rays can produce an image on a photosensitive film. X-rays can ionize the atoms they pass through and so they can damage cells of the human body when they interact with it. (Bushong 1993)

2.1 Theory of X-ray production:

Any X-ray tube consists of an evacuated glass tube that contains two main components, the cathode and the anode (target). X-ray photons are produced when an accelerated electron hits and interacts with an anode or target material. In the X-ray tube, the cathode (negative electrode) and the anode (positive electrode) are held at very high potential difference. The electrons as a result are accelerated from the cathode to the anode and gain a very high kinetic energy. The electrons are allowed to hit the anode with a very high energy and X-ray photons may be produced (Bushong 1993). The electrons travel with a kinetic energy given by:

$$K = \frac{1}{2}mv^2$$

2.4 (Bushong 1993)

Where m is the rest mAs of the electron and v is its velocity When the projectile electrons travel from the cathode and hit the atoms of the heavy metal anode, they interact with these atoms and transfer their kinetic energy to the target atoms. The projectile electrons interact with either the orbital electrons or the electric field of the nuclei of the target atoms. The interactions result in the conversion of the kinetic energy of the electron into thermal energy (heat) and electromagnetic energy (X-rays).(Bushong 1993).

The accelerated electron interact with the anode via any of the following three processes; excitation, ionization or bremsstrahlung. Each of these processes is discussed separately in the following section.

2.1.1 Excitation:

In this interaction (figure 2.5), the projectile electrons interact with the outer shell electrons of the target atoms, the outer shell electrons get excited and raised to higher energy levels. The outer shell electrons then immediately drop back to the normal energy state with the emission of

infrared radiation. In the X-ray tube this emitted infrared radiation heat the anode of the X-ray tube (Bushong 1993).

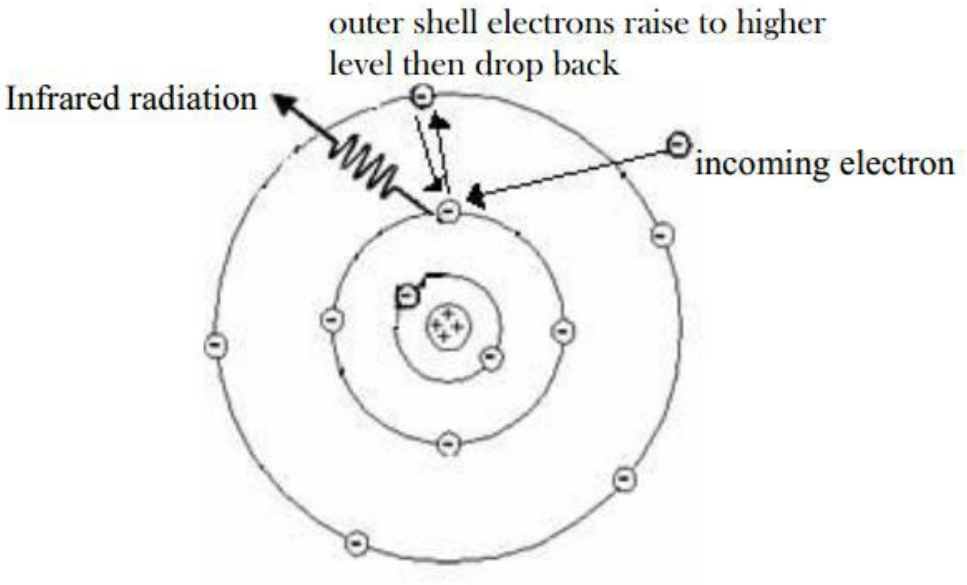

Figure 2.5 Excitation process (Bushong 1993).

2.1.2 Ionization:

In this interaction (figure 2.6), the projectile electrons interact with inner shell electrons where the energy of the incident electrons exceed the binding energy of the electrons in their shells, these inner shell electrons as a result gets ejected from their inner orbits of the target atom and the atom gets ionized and a hole is created in the place of the ejected electron. This hole is then filled by an electron from a higher energy level and characteristic X-ray lines are produced. These X-rays are called characteristic because its energy is specific to the target. (Bushong 1993).

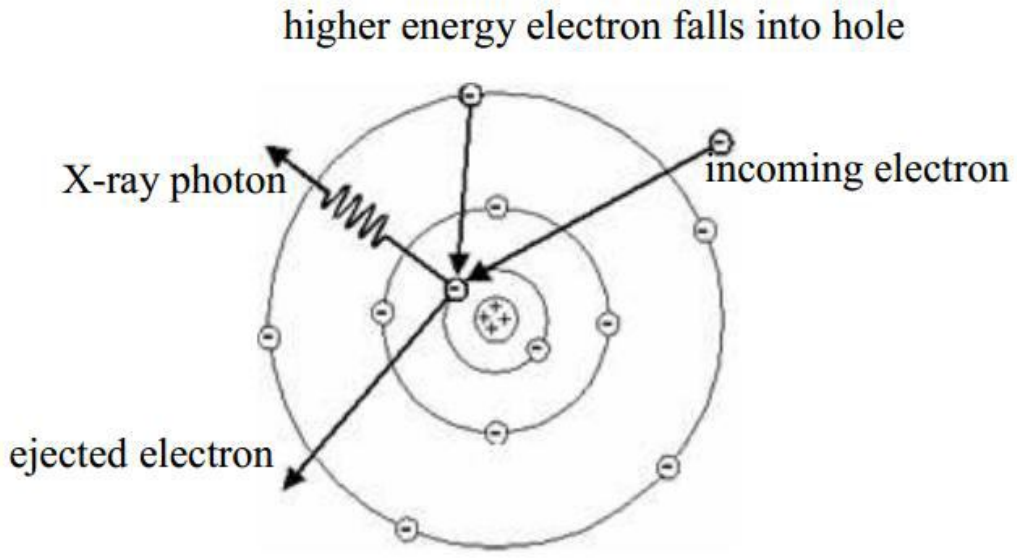

Figure 2.6 Ionization process (Bushong 1993)

2.1.3 Bremsstrahlung:

In this interaction (figure 2.7) , the electrons completely avoid the orbital electrons and come sufficiently close to the nucleus of the atom. The electrons are attracted by the strong electric field of the nucleus which causes a sudden change in the motion of the electrons and constitutes a violent deceleration that disturbs the electromagnetic field and a photon is emitted. At each interaction an X-ray is produced, which may have an energy between zero and a maximum value equal to the initial kinetic energy of the incident electron (Bushong, 1993).

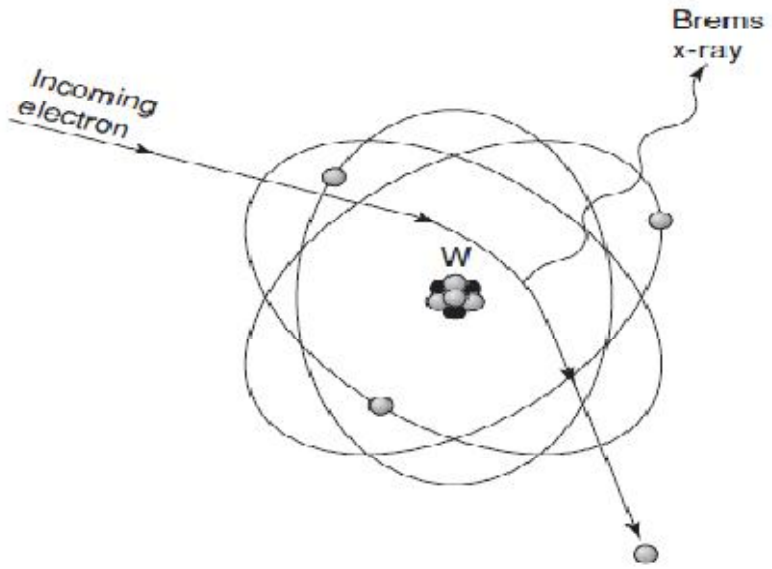

Figure 2.7 Bremsstrahlung process (Saia 2009).

2.2 X-ray spectrum and beam characteristics:

2.2.1 X-ray spectrum:

Figure 2.8 shows a typical X-ray spectrum. This spectrum consists of a continuous spectrum overlapped by number of discrete lines. The continuous spectrum represents Bremsstrahlung X-rays which have energies ranging from zero to a maximum value corresponding to the applied tube voltage. The discrete lines represent the characteristic X-rays which have precise fixed energies and that are produced by target ionization. These energies are characteristic of the differences between binding energies of the particular used element (Bushong 1993).

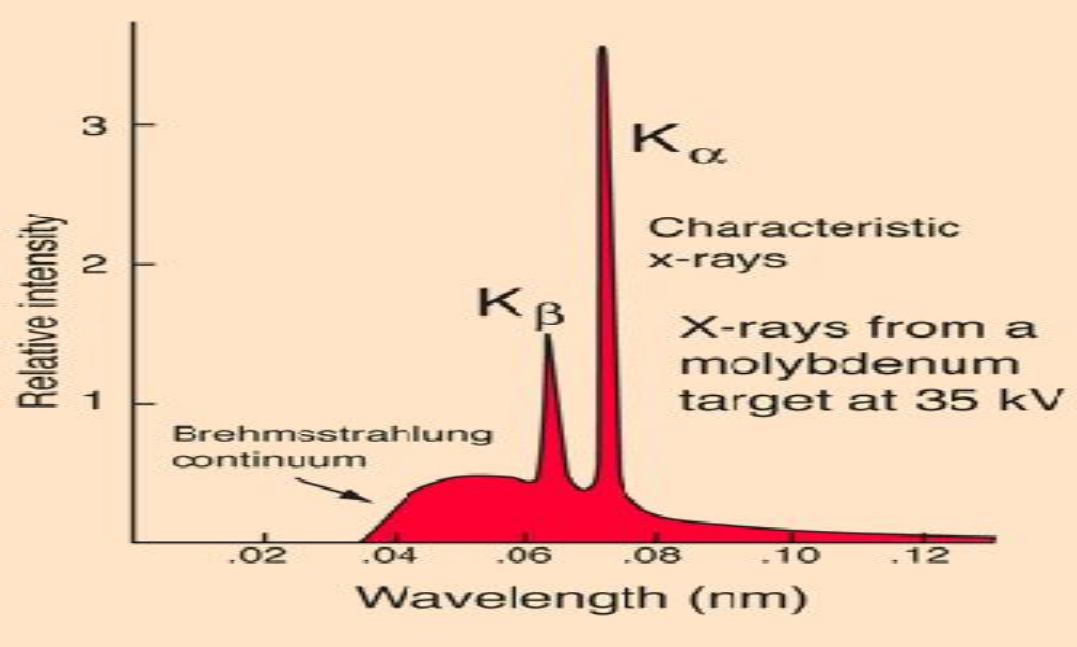

Figure 2.8: Example of X-ray spectrum (Bushong 1993)

2.2.2 X -ray beam characteristics:

X-ray beam can be described by its quality and or its quantity. Each of these characteristics is discussed separately in the following sections.

2.2.2.1 X -ray beam quantity:

The X-ray beam quantity is the X-ray intensity (number of photons per unit area per unit time) or the radiation exposure; and is affected by the change in any of the following factors: Milliampere seconds, kVps and distance and filtration.

Milliamper seconds: (mAs) is the product of X-ray tube current by the time of exposure, it controls the number of electrons accelerated towards the anode. If the current is doubled, twice as many electrons will flow from the cathode to the target, and hence twice as much X-ray photons will be produced.

Thus, X-ray quantity is directly proportional to the mAs Thus:

$$\frac{I_1}{I_2} = \frac{mAs_1}{mAs_2}$$

2.5 (Bushong 1993)

Where I_1 is the X-ray intensity that is produced when a current mAs_1, is applied on the tube, and I_2 is the X-ray intensity that is produced when current mAs_2 is applied on the X-ray tube. Thus increasing X-ray tube current will also increase X-ray quantity with the same ratio (see figure 2.9).

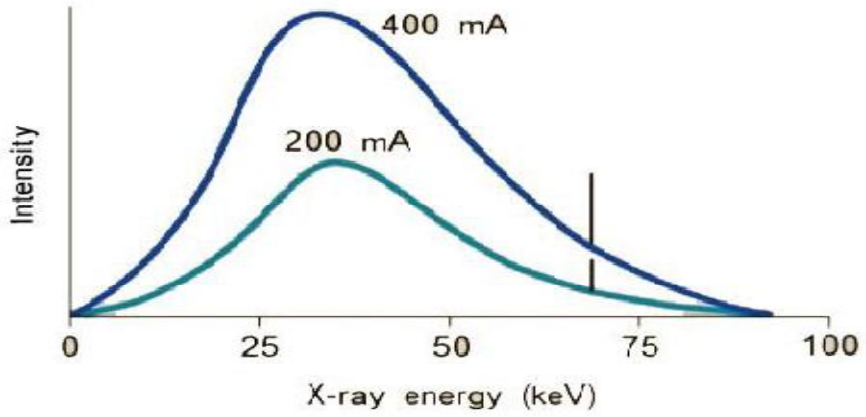

Figure 2.9: Effect of Tube current on X-ray spectrum (Hanan 2007)

Applied voltage (kVp): The increase in the applied voltage will increase the probability of bremstruhlung interaction and hence more X-ray Photons will be produced. It was found that X-ray quantity is approximately proportional to the square ratio of the applied voltage ,thus:

$$\frac{I_1}{I_2} = \left(\frac{kVp_1}{kVp_2}\right)^2$$

2.6 (Bushong 1993)

Where I_1 is the intensity of the beam produced when kVp_1 voltage is applied on the tube and I_2 is the intensity of the beam when kVp_2 voltage is applied on the tube. Any change in the potential will affect both the amplitude and the position of the X-ray spectrum. The area under the curve increases with the square of the factor by which kVp is increased and the relative distribution of emitted X-ray photons shifts to the right (higher energies)(Bushong 1993). Thus for the same mAs increasing the applied voltage will increase X-ray beam quantity.

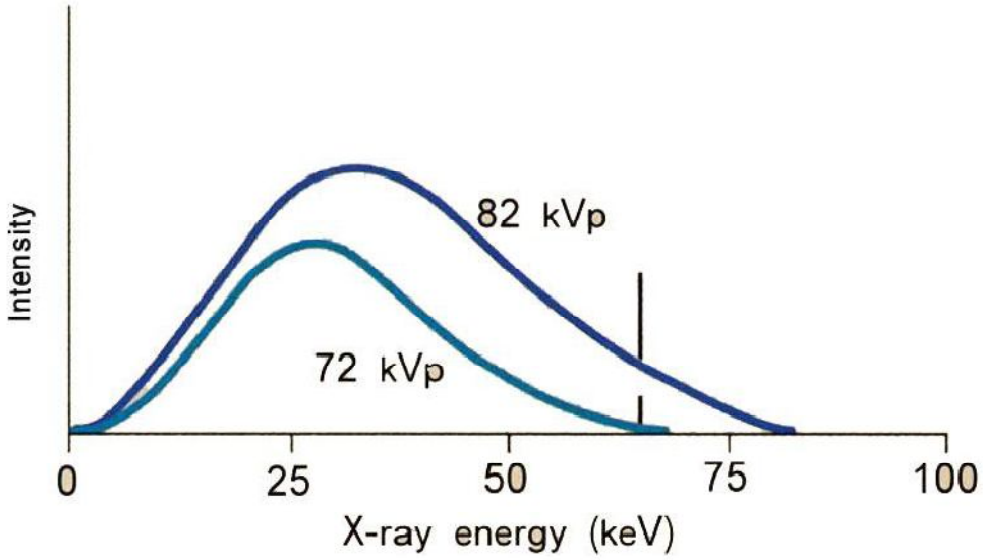

Figure 2.10: Effect of Tube potential on X-ray spectrum (Hanan 2007)

Distance: The intensity of X-rays is inversely proportional to the square distance from the target ,thus:

$$\frac{I_1}{I_2} = \left(\frac{d_2}{d_1}\right)^2$$

2.7(Bushong 1993)

where $I_1$is the intensity of the beam when a distance $d_1$is used and $I_2$is theintensity of the beam when a distance $d_2$is used Filtration: Any material that lies in the path of the X-ray beam is calledfiltration. There are two types of filtration; inherent and added filtration. The X-ray tube housing for example is an inherent filter material. Any added material to the beam is called added filtration. Filtration reduces the X-ray quantity by selectively removing low energy X-ray photons that do not add any information to the diagnosing image and hence improving the X-ray beam quality (Bushong 1993). Thus the total effect of filtration on the X-ray beams:

– Change in the X-ray spectrum shape (figure 2.11)

– The peak of the spectrum shifts towards higher energies

– The maximum energy remains unchanged

– The minimum energy shifts towards higher energies

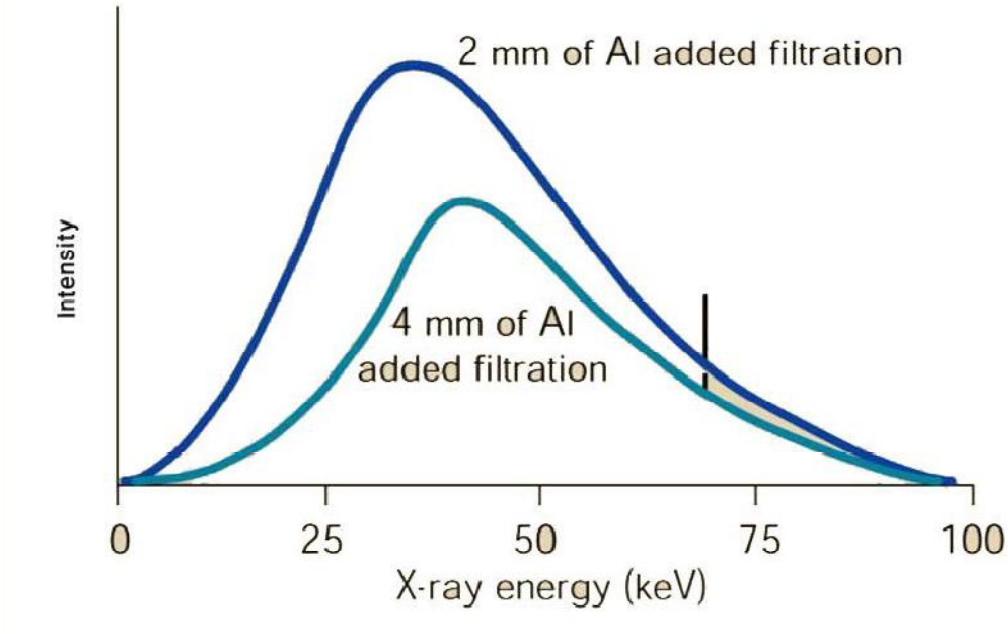

Figure 2.11 Effect of filtration on X-ray spectrum (Hanan 2007)

2.3 X-ray beam quality:

The X-ray quality is a measure of the penetrating ability of the X-ray beam and it is measured by the half value layer (HVL) of the beam. HVL is the thickness of a substance needed to reduce the intensity of the beam into half of its original value. The larger the HVL, the higher the beam quality. The following factors affect the X-ray beam quality:

Applied voltage (Kvp) The kVp controls the speed of the accelerated electrons and therefore controls the energy of the produced X-rays and the half value layer. (Bushong 1993)

Target material: The atomic number of the target material affects both the number and the effective energy of the X-rays. When the atomic number of the target is increased, the spectrum is shifted to the right . (figure 2.12) (Bushong 1993)

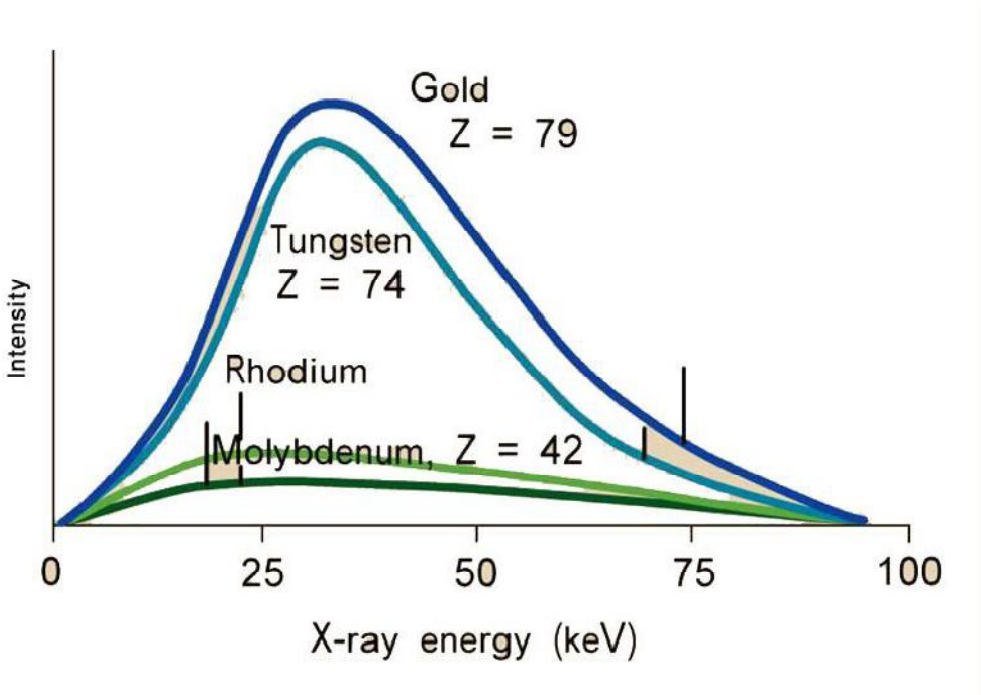

Figure 2.12: Effect of atomic number of target material on X-ray (Hanan 2007) spectrum (Tungsten atomic number = 74, Molybdenum atomic number = 42

Filtration: the increase of total filtration will increase the beam quality by removing low energy photons.

2.4 Interaction of radiation with matter:

The intensity of an x-ray beam is reduced by interaction with the matter it encounters. This attenuation results from interactions of individual photons in the beam with atoms in the absorber (patient). The x -ray photons are either absorbed or scattered out of the beam. In scattering, photons are ejected out of the primary beam as a result of interactions with the orbital electrons of absorber atoms. Four mechanisms exist where these interactions take place: Coherent scattering, Compton scattering and photoelectric absorption and pair production. In addition, about 9% of the primary photons pass through the patient without interaction to produce the image. (Curry et al.,1984)

2.4.1 Coherent Scattering:

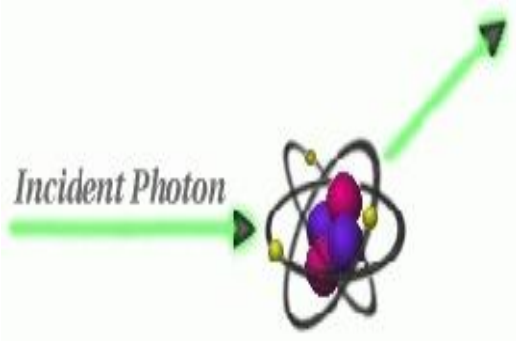

Figure 2.13: Effect Schematic diagram of classical scattering .(Curry etal.,1984)

Coherent Scattering (also known as classical scattering and Thompson Scattering) may occur when a low-energy incident photon passes near an outer electron of an atom (which has a low binding energy). The incident photon interacts with the electron in the outer-shell by causing it to vibrate momentarily at the same frequency as the incoming photon. The incident photon then ceases to exist. The vibration causes the electron to

radiate energy in the form of another x-ray photon with the same frequency and energy as in the incident photon effect. Coherent scattering contributes very little to film fog because the total quantity of scattered photons is small and its energy level is too low for much of it to reach the film. (Curry et al.,1984)

2.4.2 Compton scattering:

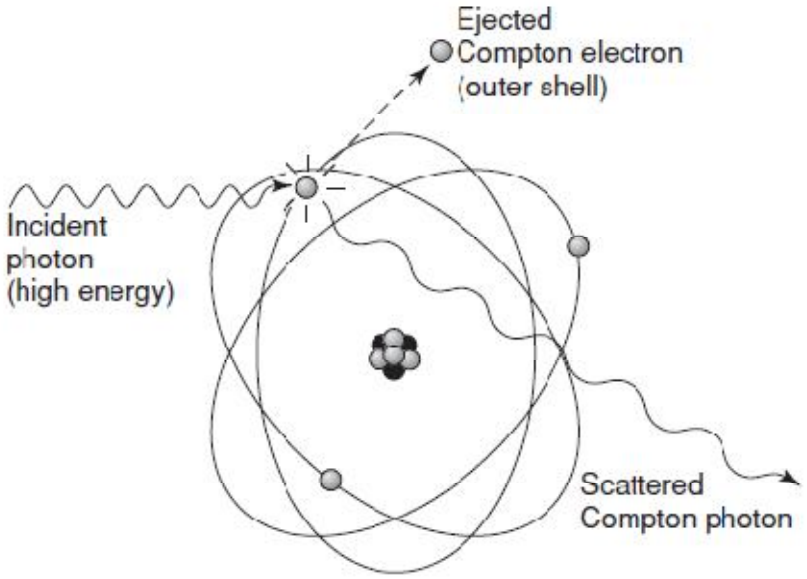

Figure 2.14: Schematic diagram of Compton scattering (Saia 2009)

Occurs when a photon interacts with an outer orbital electron, which receives kinetic energy and recoils from the point of impact. The incident photon is then deflected by its interaction and is scattered from the site of the collision. The energy of the scattered photon equals the energy of the incident photon minus the kinetic energy gained by the recoil electron plus its bonding energy. As with photoelectric absorption, Compton scattering results in the loss of an electron and ionization of the absorbing atom. Scattered photons travel in all directions. The higher the energy of the incident photon, however, the greater the probability that the angle of scatter of the secondary photon will be small and its direction will be forward. This is advantageous to the patient because some of the energy

of the incident x -ray beam escapes the tissue, but it is disadvantageous because it causes nonspecific film darkening (or fogging of the film). Scattered photons darken the film while carrying no useful information to it because their path is altered. (Curry et al., 1984) The probability of Compton scattering is directly proportional to the electron density. The number of electrons in bone is greater than in water, therefore the probability of Compton scattering is correspondingly greater in bone than in tissue. In a dental x -ray beam, approximately 62% of the photons undergo Compton scattering. (Curry et al., 1984)

The importance of photoelectric absorption and Compton scattering in diagnostic radiography relates to differences in the way photons are absorbed by various anatomic structures. The number of photoelectric and Compton interactions is greater in hard tissues than in soft tissues. As a consequence, more photons in the beam exit the patient after passing through soft tissue than through hard tissue. This allows a radiograph to provide a clear image of enamel, dentine and bone and also, soft tissue. (Curry et al,1984)

2.4.3 Photoelectric absorption:

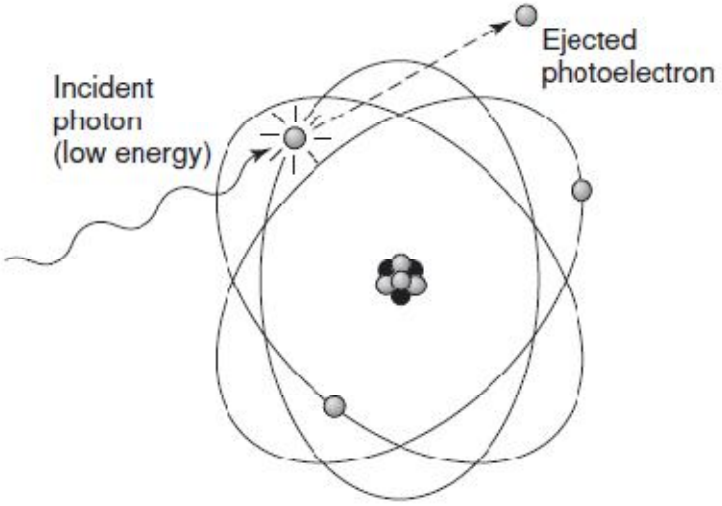

Figure 2.15: Schematic diagram of photoelectric effect (Saia 2009)

Photoelectric absorption occurs when an incident photon collides with an inner-shell electron in an atom of the absorbing medium resulting in total absorption and the incident photon ceases to exist. The electron is ejected from its shell, resulting in ionization and becomes a recoil electron (photoelectron). The kinetic energy imparted to the recoil electron is equal to the energy of the incident photon minus that used to overcome the binding energy of the electron. In the case of atoms with low atomic numbers (e.g. those in most biologic energy of the incident photon. Most Photoelectric interactions occur in the K shell because the density of the electron cloud is greater in this region and a higher probability of interaction exists. (Curry et al.,1984)

An atom that has participated in photoelectric interaction is ionized.

This electron deficiency (usually in the K shell) is instantly filled, usually by an L-or M -shell electron, with the release of characteristic radiation.

Whatever the orbit of the replacement electron, the characteristic photons generated is of such low -energy that they are absorbed within the patient and do not fog the film. (Curry et al., 1984)

The recoil electrons ejected during photoelectric absorptions travel only a short distance in the absorber before they give up t heir energy. As a consequence, all the energy of incident photons that undergo photoelectric interaction is deposited in the patient. This is beneficial in producing highquality radiographs, because no scattered radiation fogs the film, but potentially deleterious for patients because of increased radiation absorption. (Curry et al., 1984)

The frequency of photoelectric interaction varies directly with the third power of the atomic number of the absorber. For example, because the effective atomic number of compact bone (Z = 7,4), the probability that a photon will be absorbed by a photoelectric interaction in bone is approximately 6.5 times greater than in an equal distance of water. This difference is readily seen on dental radiographs. It is this difference in the absorption that makes that production of a radiographic image possible. (Curry et al., 1984)

2.4.5 Pair production:

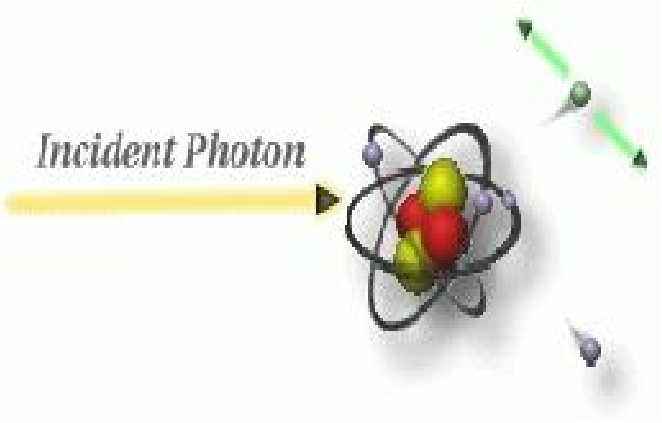

Figure 2.16: Schematic diagram of pair production (Curry et al., 1984)

In this interaction (figure 2.14) a photon with a high energy interacts with the nucleus where the photon disappears and in its place an electron positron pair appears. For this interaction to take place, the energy of the

incident photon must be at least 1.02 MeV. This is because the total rest mAs of the electron positron pair is about 1.02 MeV/c2 (Curry et al., 1984). Because its high energy, this interaction is not important in diagnostic radiology.

2.4.6 Photodisintegration:

In this interaction (figure 2.17) the incident photon has an energy greater than 10 MeV and hence it interacts directly with the nucleus and split it in parts with emission of neutrons. Because of the high photon energy required for this interaction this interaction does not occur in diagnostic X-ray and as such plays no role (Curry et al., 1984)

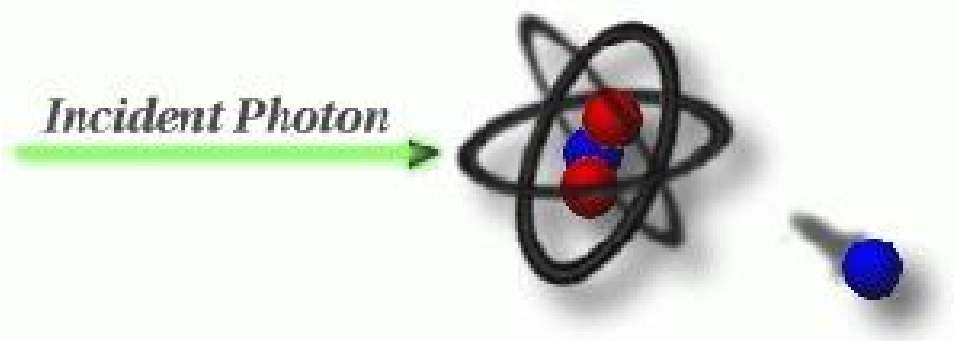

Figure 2.17: Schematic diagram of photodisintegration (Curry et al., 1984)

2.5 Radiation Quantities and Units:

Radiation dose in X-ray is classified according to the examinations that use radiation at low- dose rates. Although the risk of cancer incidence from radiation exposure with low-dose rate is lower than that high-dose rate, when a human is exposed to the same radiation dose, the International Commission on Radiation Protection (ICRP) recommends

using a dose and dose-rate effectiveness factor (DDREF). The radiation dose for each X-ray examination should be managed according to the LNT model because the risk of cancer incidence from radiation exposure on X-ray examinations cannot be excluded completely. (Br J Radiol et al.,1970)

2.5.1 Absorbed dose:

Absorbed dose is a measure of the energy deposited in a medium by ionizing radiation and is equal to the energy deposited per unit mass of medium , which is measured as joules per kilogram (J/kg) and represented by gray (Gy). When it is applied to patient dose measurement the dose is averaged over the whole volume of each tissue or organ.(Cohen BL et al., 2002)

2.5.2. Equivalent Dose:

Equivalent dose is used in radiation protection and is not measurable in practice. It accounts for the biological damage potential of different multiplying the absorbed dose for each organ or tissue by the radiation weighting factor (x- ray is defined as 1). It can be calculated from the following equation:

$$H_T = w_R D_T \qquad 2.8$$

Where H_T is the equivalent dose (in sieverts ,Sv), w_R is the radiation weighting factor , D_T is the absorbed dose for each organ or tissue.(Cohen BL et al., 2002)

2.5.3. Effective dose:

Effective dose is also used in radiation protection and is not measurable in practice. It can compare the stochastic risk of a no uniform exposure to

ionizing radiation with the risk caused by a uniform exposure of the whole body. The effective dose is obtained by calculating a weighted average of the whole-body equivalent dose to different body tissues with tissue weighting factor, which are designed to reflect the different radiosensitivities of the tissues. It can be calculated from the following equation:

$E = \sum_T w_T H_T$ 2.9(Cohen BL et al., 2002)

2.5.4 Air kerma in air:

is the sum of kinetic energy of all charged particles liberated per unit mass. A number of publications in the past have expressed measurements in terms of absorbed dose to air. Recent publications and an IAEA Code of Practice point out the experimental difficulty in determining the dose to air, especially in the vicinity of an interface, and that, in reality, what the dosimetry equipment registers is not the energy absorbed from the radiation by the air, but the energy transferred by the radiation to the charged particles resulting from the ionization. For these reasons the IAEA Code of Practice and ICRU Report 74 recommend the use of air kerma rather than absorbed dose to air. The unit is the joule per kilogram ($J\ kg^{-1}$) and is given the special name gray (Gy)

This correction applies to the quantities determined in air, such as entrance surface air kerma (rather than entrance surface air dose), computed tomography air kerma index (instead of computed tomography dose index), kerma area product (rather than dose area product) and air kerma area length (rather than dose length product).

The above recommendation refers to air. When referring to tissues, it is also correct to estimate absorbed dose to the skin, by applying the

necessary correction coefficient to obtain the absorbed dose to the tissue from the air kerma.(Br J Radiol et al.,1970)

2.6Calculation methods of entrance skin dose:

The first set of skin dose calculation was published by Birtch et al in 1974 (Birtch et al., 1979). A more simple equation of skin dose was then published by Edmond (IR Edmonds 1984) in 1984. Edmonds used the data published by Birtch and proved that these radiation doses can be reduced to a simple function that depends on kVp, mAs, filtration and SSD. Edmonds noted that skin dose is proportional to (kVp)1.74 and as such , skin dose may be given by. (Birtch et al., 1979).

$$skin-dose(\mu Gy)=\frac{836(kVp)^{1.74}(mAs)}{(SSD)^2}(\frac{1}{T}+0.114) \qquad 2.10$$

Where T is the total filtration in mm Aluminum, SSD is the source to skin distance in cm, and kVp is the applied kilo voltage. The second studies by Shrimpton (Shrimpton 1985) who compared the results obtained using Edmonds formula with that obtained by direct measurement of skin dose using TLD. Shrimpton noted that Edmond's formula produce an estimate of air kerma in the absence of patients, and its use in estimating skin dose may involve significant error. The second trace of skin dose can be found in the literature was the two formulas published by Tung and Tsai in 1999 (Tung et al., 1999). Similar to the approach used by Edmonds (Edmonds 1984), Tung and Tsai studied the relationship between 34 entrance skin dose and X-ray tube potential and between entrance skin dose and Aluminum filtration. These two relations allowed Tung and Tsai to propose the followingequation for three phase X-ray generators:

$$ESD = c\left(\frac{KVp}{FSD}\right)^2\left(\frac{mAs}{mm.Al}\right) \qquad 2.11$$

Where ESD is the entrance skin dose, kVp is the applied tube potential, mAs is the applied mAs (tube current multiplied by exposure time), FSD is the focus to skin distance, and c is the proportionality constant or machine dependant constant which depends on the X-ray machine and is about 2.775 for all manufacturers and X-ray machines studied by Tong and Tsai. Also the dose may calculate by the dose calculation system that designed to calculate and report entrance surface dose. By determining the tube output data and exposure factors encountered. Using equation 1.(Suliman 2008).

$$ESD = OPx\left(\frac{kV}{80}\right)^2 xmAsx\left(\frac{100}{FSD}\right)^2 xBSF \qquad 2.12$$

Where (OP) is the output in mGy/ (mA s) of the X-ray tube at 80 kV at a focus distance of 1 m normalized to 10 mA s, (kV) the tube potential, (mA s) the product of the tube current (in mA) and the exposure time(in s), (FSD) the focus-to-skin distance (in cm) and (BSF) the backscatter factor. The normalization at80 kV and 10 mA s was used as the potentials across the X-ray tube and the tube current are highly stabilized at thispoint.BSF is calculated automatically by the Dose Cal software after all input data are entered manually in the software. The tube output, the patient anthropometrical data and the radiographic parameters (kVp, mA s, FSD and filtration) are initially inserted in the software. The kinds of examination and projection are selected afterwards. (Tung et al., 1999).

2.7 Previous data:

Ocena et al , 2014study X-ray examination that associated with patient exposure to ionizing radiation. Dose values depend on the type of medical procedure used, the X-ray unit technical condition and exposure conditions selected. The aim of this study was to determine the dose value received by patients during certain conventional radiography X-ray examinations and to assess the technical condition of medical equipment used for this purpose. Material and Methods: The study covered the total number of 118 conventional diagnostic X-ray units located in the MasovianVoivodeship. The methodology used to assess the conventional diagnostic X-ray unit technical condition and the measurement of the radiation dose rate received by patients are based on test procedures developed by the Department of Radiation Protection and Radiobiology of the National Institute of Public Health – National Institute of Hygiene (Warszawa, Poland) accredited for compliance with PN-EN 17025 standard by the Polish Centre for Accreditation. Results: It was found that 84.7% of X-ray units fully meet the criteria set out in the Polish legislation regarding the safe use of ionizing radiation in medicine, while 15.3% of the units do not meet some of them. The broadest dose value range was recorded for adult patients. Particularly, during lateral (LAT) lumbar spine radiography the recorded entrance surface dose (ESD) values ranged from 283.5 to 7827 μGy (mean: 2183.3 μGy). Conclusions: It is absolutely necessary to constantly monitor the technical condition of all X-ray units, because it affects population exposure to ionizing radiation. Furthermore, it is essential to raise radiographers' awareness of the effects that ionizing radiation exposure can have on the human body. (OCENA etDegree,al, 2014.

EhsanMoudi et al 2014 study Panoramic imaging is one of the most commonly used imaging techniques in dentistry. Being able to accurately assess the radiation dose patients receive during procedures is a crucial step in the management of dose. The main objective of this study was to evaluate the head and neck skin absorbed dose during panoramic radiography in different age groups with panoramic machine of Oral and Maxillofacial Radiology section of Babolschool of dentistry. Materials and methods: 273 thermoluminescentdosemeters (TLDs) (100 LiF: Mg, Ti ,harshaw, USA) were used.90 samples were selected from the patients who referred to the Oral and Maxillofacial Radiology section of Babol school of dentistry for panoramic radiography. .Samples divided in 3 age_ group: 4_ 10 years, 10_40 years and above 40 years . TLDs were calibrated in dosimetry laboratory, National Radiation Protection Department. Thermoluminescent signal was read out with a Harshaw 4500 (Harshaw, Bicron USA) reader. Mean and standard deviation was determined by SPSS10 software and ANOVA statistical analysis.

Mean ± SD of skin absorbed dose of head and neck for 90 patients was 0.47Degree± 0.09mGy. Conclusions:

Since Degreeof Reference level (DRL) of panoramic imaging is unknown in Iran, there is no possibility to compare the current results with DRL. However, this study conclude that decrease of radiation dose seems to be achievable with lower exposure condition with the panoramic unit.EDegreehsan(Moudi et.al) Degree

Bouzarjomehri et al2007 ,Radiation dose knowledge through Xray examinations and their distribution provides useful guidance on patient dose reduction. The results of the entrance skin dose (ESDs) of five common radiographies in all radiology centers in Yazd province were reported in our previous study (2003). In the present study we have evaluated the collective effective dose of conventional X-ray

examinations, as well as the annual per caput of Yazd population. *Materials and Methods:* The annual frequencies of 18 different types of conventional radiology examinations during April 2005 to March 2006 were recorded from all 35 radiology centers in Yazd province. The exposure conditions consisted of kVp, mAs, and Focus surface distance (FSD) of the examinations for the mode of exposure in each X-ray unit. 620 ESD were measured by diode dosimeter in 35 hospitals and clinics. The real exposure kVp for each radiology unit was measured by a Molt-O-Meter. The conversion coefficient (effective dose - ESD ratio) for each radiology examination was determined by using SR262 tables. Finally, the patients' effective dose was calculated by multiplying the conversion factor to the ESD. *Results:* The patients' annual collective effective dose due to the conventional radiology examinations was 31.159 man-Sv (0.03 mSv per inhabitant). The frequency of examinations was 311813 i.e. 0.36 examinations per head of the population for one year.

Conclusion: According to our findings, the effective per caput dose seems to be optimally relative to HCL-II countries, which may be due to low mean effective dose that could obscure high examination frequency. The number of radiology conventional examinations and frequency of radiologist per1000 population of Yazd was more and lower than HCL-II countries respectively. Thus the justification of radiography requests in this province must be revised. (F. et al ., 2007.

Ademolaetal., 2013 study Assessment of Entrance Skin Dose in routine x-ray examinationsof chest, skull, abdomen and pelvis of children in five selected hospitals in Nigeria this study assumed that children are more susceptible to the effects of ionizing radiation and so deserves special attention. Entrance skin doses (ESD) and Effective dose (E) to pediatric patients were estimated during chest, skull, abdomen and pelvis examination in five Nigeria hospitals using DoseCal software. The mean

ESD for Chest (PA) in age range 1 – 5 in the five hospitals (H1 – H5) were 70, 139, 130, 105 and 111μGy, respectively. The median ESD values in all the examinations were compared with the NRPB and EC reference level and were found to be lower except for Chest PA and Chest Lateral examinations. The mean effective doses were compared with those found in literature and were found to be comparable. (Ademolaetal., 2013).

CHAPTER THREE

3. Materials and Method

3.1 Materials:

3.1.1 The machine used:

Machines that used in this study are:

SHIMADZU model0.6\1.2p18DE-85 Manufactured in May 2011 in japan, SHIMADZU ,model R-20j,Manufactured in January 2010 in japan,SHIMADZU ,model collimator R-20j,Manufactured in June 2008 in japan,SHIMADZU ,model 1.2u161cs-31 ,Manufactured in may 2008 in japan

3.1.2 Place of the study:

This study conducted in Red Sea State in four hospital and they are:

-Customhouses clinic,police hospital port Sudan, Health insurance centre port Sudan andsea port corporation hospital

3.1.3Population of the study:

The study includes patients with X-ray investigation for all ages, gender and ethnic groups.

3.1.4 Study sample:

A total of 146 patients will be included in this study. The data will include patient weight, height, tube current, tube voltage, time product setting. The absorbed dose will be measured for thoraco-lumbar and skull examinations.

3.2 Method

3.2.1 Dose calculation:

In order to increase the speed and efficiency of the patient dosimetry process, windows-based computer program, CALDose_X 5.0, which is developed by Kramer et al (2008)., was used in the present study.

CALDose_X 5.0 is a software tool that enables the calculation of the Incident Air Kerma (INAK) based on the output curve of an x-ray tube and of the Entrance surface air kerma (ESAK) by multiplying the INAK with a backscatter factor, as well as organ and tissue absorbed doses and effective doses for posture-specific female and a male adult phantoms, using conversion coefficients (CCs) normalized to the INAK, the ESAK or the Air Kerma Area Product (AKAP) for examinations frequently performed in X-ray diagnosis.

3.2.2 Data analysis:

Analysis of data doneusing Microsoft Excel and SPSS software .

Chapter Four

Table 4.1 show demographic data for all patients in thoraco-lumber x.ray examinations.

	Age	Weight	High	KVp	MAs	INAK	ESAK	RCI	MaxBSC absorbed dose	Weighted Mash dose
Mean	42.47	76.15	168.44	79.41	43.62	0.5245	0.7309	1.04110	0.46635	0.24795
STD	13.955	10.837	8.059	5.103	9.059	0.14157	0.20411	0.752906	0.153747	0.081817
Min	18	54	148	70	28	0.28	0.39	0.030	0.236	0.117
Max	75	112	189	95	58	0.89	1.28	3.034	0.909	0.489

Table 4.2 show correlations between weight, INAK and Mash dose from thoraco-lumber examinations.

Correlations

		Weight	Incident air kerma	WEIGHTED MASH DOSE
Weight	Pearson Correlation	1	.659**	.670**
	Sig. (2-tailed)		.000	.000
	N	78	78	78
Incident air kerma	Pearson Correlation	.659**	1	.993**
	Sig. (2-tailed)	.000		.000
	N	78	78	78
WEIGHTED MASH DOSE	Pearson Correlation	.670**	.993**	1
	Sig. (2-tailed)	.000	.000	
	N	78	78	78

**. Correlation is significant at the 0.01 level (2-tailed).

Figure 4.1 show box plot for mean from all hospital forthoraco-lumber examinations.

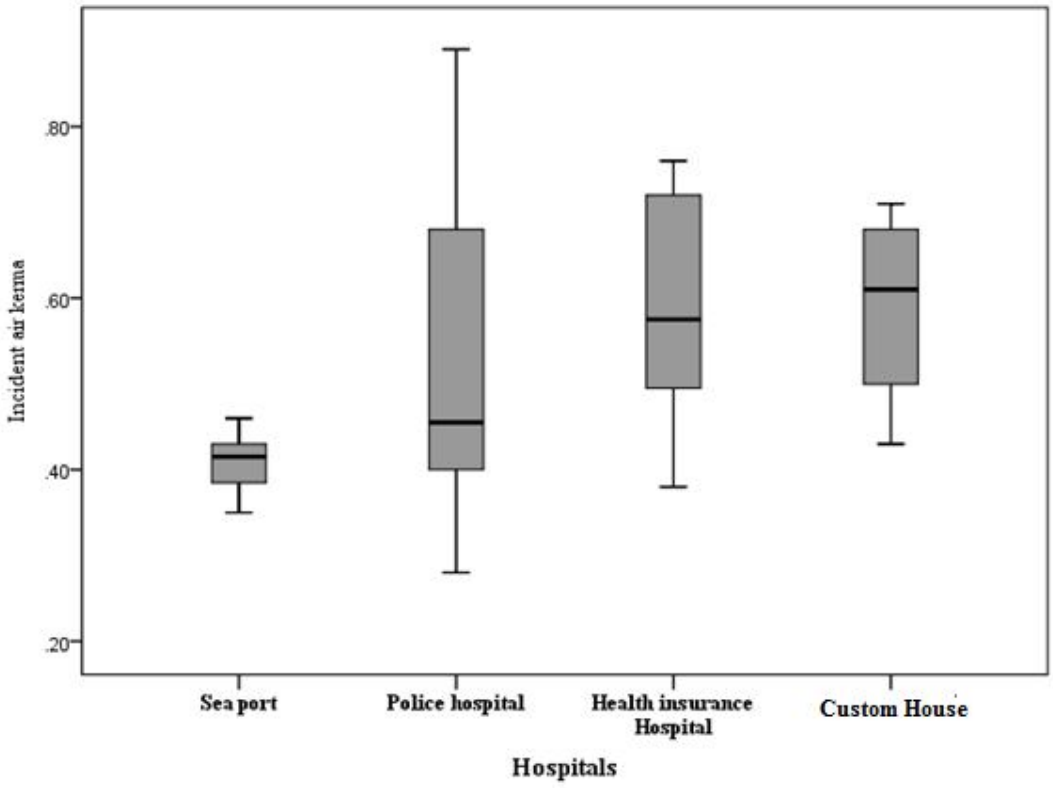

Table 4.3 shows descriptive statistical for INAK to thoraco-lumber examinations.

Descriptive

Incident air kerma

	N	Mean	Std. Deviation	Std. Error	95% Confidence Interval for Mean		Minimum	Maximum
					Lower Bound	Upper Bound		
Sea port	20	.4085	.03329	.00744	.3929	.4241	.35	.46
Police hospital	20	.5295	.19132	.04278	.4400	.6190	.28	.89
Health insurance Hospital	20	.5800	.11675	.02611	.5254	.6346	.38	.76
Custom house Hospital	18	.5861	.09948	.02345	.5366	.6356	.43	.71
Total	78	.5245	.14157	.01603	.4926	.5564	.28	.89

Table 4.4 show multiple comparison between hospitals for Incident air kerma:

(I) Hospitals	(J) Hospitals	Mean Difference (I-J)	Std. Error	Sig.	95% Confidence Interval	
					Lower Bound	Upper Bound
Sea port	Police hospital	-.12100*	.03931	.015	-.2243	-.0177
	Health insurance Hospital	-.17150*	.03931	.000	-.2748	-.0682
	Custom house Hospital	-.17761*	.04039	.000	-.2838	-.0714
Police hospital	Sea port	.12100*	.03931	.015	.0177	.2243
	Health insurance Hospital	-.05050	.03931	.576	-.1538	.0528
	Custom house Hospital	-.05661	.04039	.502	-.1628	.0496
Health insurance Hospital	Sea port	.17150*	.03931	.000	.0682	.2748
	Police hospital	.05050	.03931	.576	-.0528	.1538
	Custom house Hospital	-.00611	.04039	.999	-.1123	.1001
Custom house Hospital	Sea port	.17761*	.04039	.000	.0714	.2838
	Police hospital	.05661	.04039	.502	-.0496	.1628
	Health insurance Hospital	.00611	.04039	.999	-.1001	.1123

*. The mean difference is significant at the 0.05 level.

Table 4.5 show demographic data for all patients in skull x.ray examinations.

	Age	Weight	High	KVp	MAs	INAK	ESAK	RCI	Max BSC absorbed dose	Weighted Mash dose
Mean	39.28	72.71	167.71	64.12	15.26	0.6751	0.7948	0.3940	0.2250	0.0145
STD	14.725	10.025	7.217	4.833	4.120	0.25561	0.30649	0.19475	0.09675	0.00530
Min	20	55	149	54	9	0.27	0.33	0.11	0.08	0.00
Max	72	105	181	70	20	1.00	1.22	0.79	0.37	0.02

Table 4.6 show correlations between weight, ESAK and MAXIMUM BSC ABSORBED DOSEfrom skullx.ray examination.

Correlations

		Weight	MAXIMUM BSC ABSORBED DOSE	Entrance Surface air Kerma
Weight	Pearson Correlation	1	.056	.045
	Sig. (2-tailed)		.647	.717
	N	68	68	68
MAXIMUM BSC ABSORBED DOSE	Pearson Correlation	.056	1	.996**
	Sig. (2-tailed)	.647		.000
	N	68	68	68
Entrance Surface air Kerma	Pearson Correlation	.045	.996**	1
	Sig. (2-tailed)	.717	.000	
	N	68	68	68

**. Correlation is significant at the 0.01 level (2-tailed).

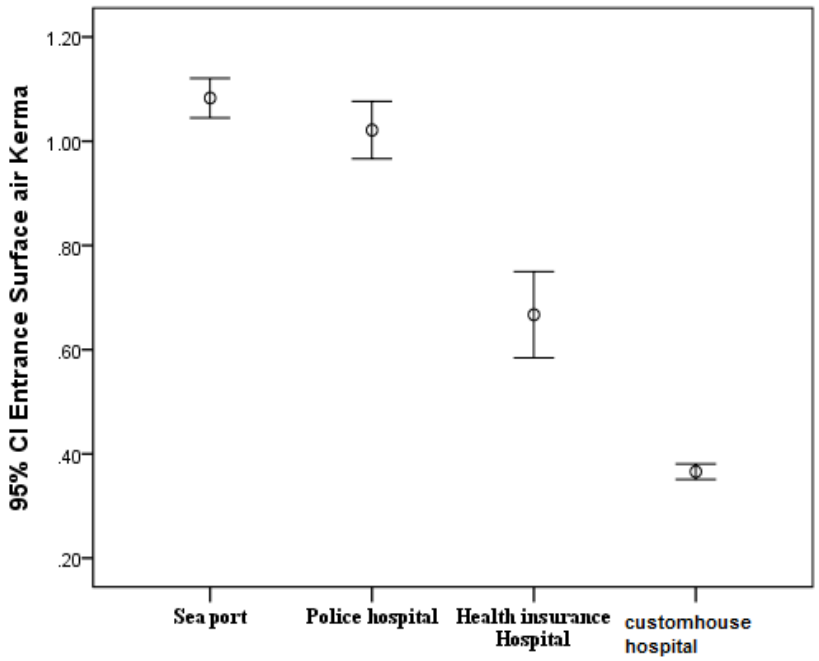

Figure 4.2 show box plot for mean from all hospital for skull examinations

Table 4.7 show descriptive statistical descriptive for ESAK to skull x.ray examination.

Descriptives

Entrance Surface air Kerma

	N	Mean	Std. Deviation	Std. Error	95% Confidence Interval for Mean		Minimum	Maximum
					Lower Bound	Upper Bound		
Sea port	18	1.0828	.07629	.01798	1.0449	1.1208	.94	1.22
Police hospital	17	1.0213	.10711	.02598	.9662	1.0764	.86	1.18
Health insurance Hospital	17	.6671	.16097	.03904	.5844	.7499	.42	.90
Custom house Hospital	16	.3659	.02754	.00689	.3513	.3806	.33	.42
Total	68	.7948	.30649	.03717	.7207	.8690	.33	1.22

Table 4.8 shows multiple comparisons between hospitals for Entrance Surface air Kerma:

(I) Hospitals	(J) Hospitals	Mean Difference (I-J)	Std. Error	Sig.	95% Confidence Interval	
					Lower Bound	Upper Bound
Sea port	Police hospital	.06154	.03558	.317	-.0323	.1554
	Health insurance Hospital	.41572*	.03558	.000	.3219	.5096
	Custom house Hospital	.71690*	.03615	.000	.6215	.8123
Police hospital	Sea port	-.06154	.03558	.317	-.1554	.0323
	Health insurance Hospital	.35418*	.03609	.000	.2590	.4494
	Custom house Hospital	.65536*	.03665	.000	.5587	.7520
Health insurance Hospital	Sea port	-.41572*	.03558	.000	-.5096	-.3219
	Police hospital	-.35418*	.03609	.000	-.4494	-.2590
	Custom house Hospital	.30118*	.03665	.000	.2045	.3979
Custom house Hospital	Sea port	-.71690*	.03615	.000	-.8123	-.6215
	Police hospital	-.65536*	.03665	.000	-.7520	-.5587
	Health insurance Hospital	-.30118*	.03665	.000	-.3979	-.2045

*. The mean difference is significant at the 0.05 level.

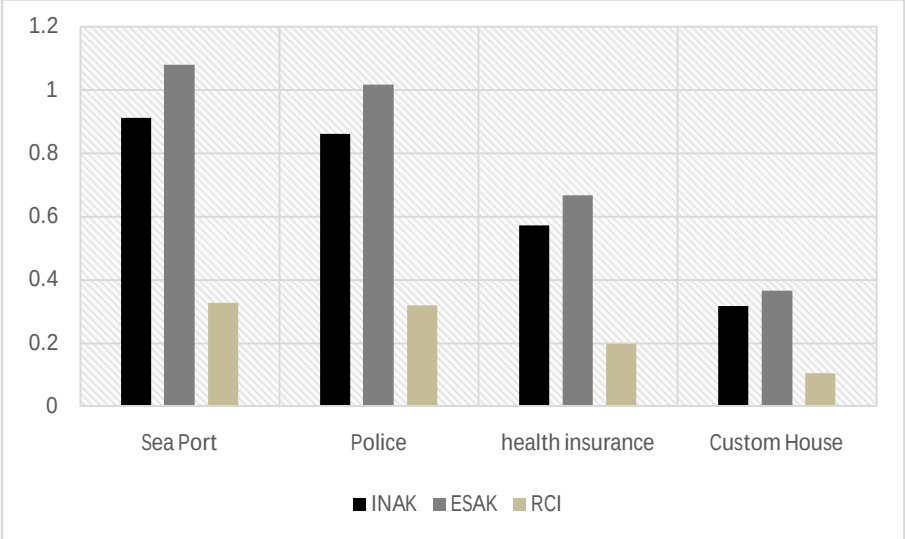

Figure 4.3 show compare between INAK, ESAK and RCI for skull x.ray examinations to all hospitals.

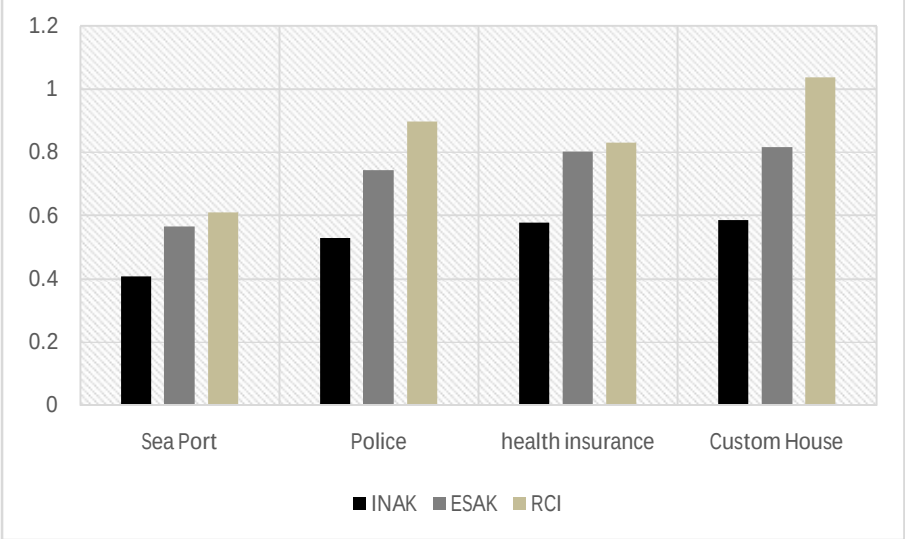

Figure 4.4 show compare between INAK, ESAK and RCI for thoraco-lumber x.ray examinations to allhospitals.

Table 4.9 show compare between present study and DRLs.

Organ	Present study	UK 2000	CRCPD 1988	IAEA 1996	EU 1996	NRPB 1999	SCG 2005
Skull	0.7948	2.25	1.3	4	4	3	4.25
Th.L	0.7309	12.75	-	13.5	_	10.5	8.85

Chapter five

Discussion, conclusion and recommendation

5.1 Discussion:

In this study a total of 146 adult patient examined to thoraco- lumbr and skull x-ray exam in police hospital, health insurance center, customhouse hospital and sea port hospital.

The result of this study showed wide variation in patient among different hospitals in term of entrance surface air kerma (ESAK), incidence air kerma (INAK)and the risk of cancer incidence (RCI). This might be due to operator'sperformance and status of machine.

The result of the study revealed that the Kvp used ranged from (70-95) (79.41±5.103), mAs ranged from (28-58) (43.62±9.059),for INAK ranged from (0.28-0.89) mGY (0.5245±0.14157),for ESAK ranged from (0.39-1.28) mGY (0.3709±0.20411), for RCI ranged from (0.030-3.034) (1.0411±0.7529), for maximum BSC absorbed dose ranged from (0.236-0.909) mGY (0.46635±0.153747) and for weighted Mash dose ranged from (0.117-0.489) mGy(0.24795±0.081817), this result found to be at the normal range of dose reference level

Correlation between three variables weight incidence air kema and weighted Mash dose was studied, it showed significant correlation ($p<0.01$).

error bar plot between all hospital for patient examined to thoraco-lumbar and found then is different in INAK values between hospitals.

descriptive statistic for INAK to thoraco- lumbar x-ray examinations which they mean, STD, STD error and 95% confidence interval for mean

to lower bound, upper bound, minimum and maximum values for all hospitals .

multi comparison between all hospitals using INAK by mean difference, STD error, significant and confidence interval .

The result of the study revealed that the age were ranged from (20-72) years and (39.28±14.725) , FOR weight were ranged from (55-105) kilograms (72.71±10.025),for height ranged from (149-181) centimeters (167.71±7.217) ,for KVP ranged from (54-70) kilovolt (64.12±4.833), for mAs ranged from (9-20) mille ampere (15.26±4.120),for INAK ranged from (0.27-1.0) mGY (0.6751±0.25561),for ESAK ranged from (0.33-1.22) mGY (0.7948±0.30649), for RCI ranged from (0.11-0.79) (0.3940±0.19475), for maximum BSC absorbed dose ranged from (0.08-0.37) mGY (0.2250±0.09675) and for weighted Mash dose ranged from (0.00-0.02) mGY (0.0145±0.00530).this result found to be at the normal range of dose reference level .

Correlation between three variables weight, ESAK and maximum BSC absorbed dose was studied, it showed significant correlation ($p<0.01$).

error bar plot between all hospital for patient examined to skull and found then is different in ESAK values between hospitals.

descriptive statistic for ESAK to skull x-ray examinations which they mean, STD, STD error and 95% confidence interval for mean to lower bound, upper bound, minimum and maximum values for all hospitals .

multi comparison between all hospitals using ESAK by mean difference, STD error, significant and confidence interval .

compare between INAK, ESAK and RCI for skull x.ray examinations to all hospitals, whereas INAK was higher in seaport hospital and lower in

customhouse hospital, ESAK was higher in seaport hospital and lower in customhouse hospital and RCI was higher in seaport hospital and lower in customhouse hospital.

compare between INAK, ESAK and RCI for thoraco- lumber x.ray examinations to all hospitals, , whereas INAK was higher in customhouse and health insurance and lower in seaport hospital, ESAK was higher in customhouse hospital and lower in seaport hospital and RCI was higher in customhouse hospital and lower in seaport hospital.

compare between present study and DRLs, the dose found in this study was lower than the reported by international organization and DRLs.

5.2 Conclusion

This study design to assessment of patient dose during x-ray examination in Red Sea state to skull and thoraco- lumbar examination.

The patient dose done in seaport hospital, health insurance center, police hospital and customhouse hospital, and found the dose for thoraco-lumbar examinations higher in seaport hospital and for skull examinations higher in customhouse hospital.

The finding from present study showed that optimization of technical and clinical factors may lead to a substantial patient dose reduction. And the present study measure that the dose much lower than the reference level that recommended by international organization .

5.3 Recommendation:

Radiology department should implement a patient dose measurement and quality assurance program.

Dose to patient should be regularly monitored and the proposed national DRLs should be taken as guidance for optimization.

X-ray machine must be used with high level of training for medical staff due to the high dose.

REFERENCES

AdemolaIOSRJournalofAppliedPhysics(IOSR-JAP)e-ISSN:22784861.Volume5, Issue2(Nov.-Dec.2013),PP47-50.Annals oftheICRP:RisksassociatedwithionizingradiationsRisksassociatedwithio nizingradiationsRisksassociatedwith ionizingradiations.Oxford:PergamonPress;1991b;22(1).

AssessmentofEntranceSkinDoseandEffectiveDoseofSomeRoutineX-rayExaminationsUsingCalculationTechnique.

BirtchR,MaeshallM:Computationofbremsstrahlungx-rayspectrameasuredwithGe(Li)detectorandcomparisonspectrameasuredw ithGe(Li)detector.PhsMedBiol1979;24:505-517.

BushongSC:RadiographicScienceforTechnologists: Physics,RadiographicScienceforTechnologists:Physics,Biology,andProte ction,Biology,andProtection,5th Edition. St. Louis, MO: Mosby-YearBook,1993.

Cohen BL (2002) Cancer risk from low level radiation. AJR179:1137–1143.

Curry TS, Dowdey JE, Murry RC: Christensen's Introduction to the Christensen's Introduction to the physics of Diagnostic Radiology physics of Diagnostic Radiology. 3rd ed. Lea &Febiger, Philadelphia, PA, 1984.

D.A. Saia, MA, RT(R) (M) Director, Radiography Program Stamford Hospital Stamford, Connecticut, ed 5, 2009.

EC McCullough and JR Cameron: Exposure rates from diagnostic X-ray units ray units, Br J Radiol 1970 43: 448-449

European Committee, EC. (1996). European guidelines on quality criteria for diagnostic radiographic images. EUR 16260EN National Radiologic Protection Board. (2000).

ICRP Publication 73, Radiological protection and safety in medicine, Ann, ICRP 26(2) 1996.

International Atomic Agency: International basic safety standards for for protection against ionizing radiation and for safety of radiation sources. IAEA Safety Series No. 115-1, IAEA, Vienna1994.

International Atomic Energy Agency.(1996) International basic standards for protection against ionizing radiation and for the safety of radiation source. Vienna: IAEA Safety Series.

International Commission on Radiological Protection, ICRP: Recommendations of the ICRP recommendations of the ICRP, ICRP publication 60. Annuals of the ICRP.Pergamon Oxford. 1991.

PC Shrimpton: Calculation of patient skin dose from diagnostic X –ray procedures , Br J Radiol 1985 58: 483-485.

Radiological protection and safety in medicine Radiological protection and safety in medicine.ICRP publication 73.Annuals of the ICRP. Oxford: Pergamon Press; 1996b;26 (2).

Suliman, I.I., Abbas, N. and Habbani, F.I. (2007) Entrance Surface Doses to Patients Undergoing Selected Diagnostic X-Ray Examinations in Sudan. Radiation Protection Dosimetry, 123, 209-214. http://dx.doi.org/10.1093/rpd/ncl137.